# Robust Self-Healing Host–Guest Gels from Magnetocaloric Radical Polymerization

*Chao Yu, Cai-Feng Wang,* and Su Chen**

**Given the increasing environmental and energy issues, materials with the ability to repair themselves following damage are highly desirable because this self-healing property can prolong the lifespan of materials and reduce replacement costs. Host–guest assemblies are a powerful approach to create supramolecular materials with versatile functions. Here, a new mode of radical polymerization is demonstrated which is achieved via magnetocaloric effect to fabricate novel host–guest supramolecular gels within 5 min. The resulting gels can repair themselves spontaneously when damaged, without the assistance of any external stimuli, and possess great mechanical strength. Moreover, the $Fe_3O_4$-doped supramolecular gels show accelerated self-healing (from 24 h to 3 h) under an applied magnetic field, which is attributed to the synergy between host–guest healing and a magnetocaloric effect. This strategy might open a promising avenue for accelerating the use of host–guest assemblies to rapidly build robust materials.**

## 1. Introduction

Self-healing exists widely in living organisms, from micro blood clotting to macro skin repair. This special biological process benefits living organisms to restore their integrity and prolongs their lifespan. To mimic such natural healing feature, a variety of smart materials have been exploited on the basis of various strategies,[1–8] involving release of healing agents, stimuli response, covalent cross-links and supramolecular assembly. Of particular interest among those reported is supramolecular system, which is actively involved in biochemical process and is closely approximate to the life entity.[9] Generally, in such system non-covalent interactions such as $\pi$–$\pi$ stacking,[10,11] hydrogen bond,[12,13] electrostatic interaction,[14,15] and hydrophobic interactions[16,17] are utilized to harness a healing response. Nevertheless, maintenance-free polymers with supermolecular networks constructed by host–guest complementarity are still rarely reported.[18–20] Moreover, it is still a great challenge to fabricate supramolecular materials with both superior self-healing and mechanical performance, since there seems an inherent compromise between these two properties that dynamic healing benefits from weak interactions but strong interactions give mechanical strength.[13]

Herein, $\beta$-cyclodextrin (CD),[21–25] an eco-friendly and affordable "host", was introduced to combine with a "guest" *N*-vinylimidazole (VI) to synthesize $Fe_3O_4$-doped self-healing gels with great mechanical strength through the first implementation of a new mode of radical polymerization, magnetically induced frontal polymerization (MIFP). This work has the following notable characteristics: (1) developing a new mode of radical polymerization that takes full advantage of magnetocaloric effect (also known as magnetic hyperthermia)[26–29] to ignite the polymerization to fast synthesize targeted products in minutes; (2) exploring new auto-healing supermolecular gels with high performance. Most achievements to self-healing materials reported previously require the input of external stimuli. Without any treatment, the supramolecular gels possessing great mechanical strength developed herein can heal themselves spontaneously, representing the rare examples of synthetic materials with combination of intrinsic self-healing capability and superior mechanical performance; (3) utilizing the synergy between host-guest healing and magnetocaloric effect to greatly speed the wound-repair process from 24 h to 3 h, which has never been described before. Thus, this work demonstrates a new simple and low-energy pathway to fabricate versatile self-healing materials with desired performance, which can also be extended to explore diverse functional polymer composites.

## 2. Results and Discussion

### 2.1. Preparation of Supramolecular Gels

The schematic procedure for rapid (within 5 min) fabrication of supramolecular gels via MIFP is shown in **Figure 1**. $Fe_3O_4$ nanoparticles with superparamagnetism (see Supporting Information Figure S1) were dispersed into a mixture of CD, VI, 2-hydroxypropyl acrylate (HPA), ammonium persulfate (APS)/*N,N,N′,N′*-tetramethylethylenediamine (TMEDA) (redox initiator) and methylenebisacrylamide (MBAA, crosslinker). After being triggered via an external magnetic field for several seconds, a travelling "Front" considered as the boundary

C. Yu, Dr. C.-F. Wang, Prof. S. Chen
State Key Laboratory of Materials-Oriented Chemical Engineering and College of Chemistry and Chemical Engineering
Nanjing University of Technology
Nanjing, 210009, PR China
E-mail: caifengwang@njut.edu.cn; chensu@njut.edu.cn

DOI: 10.1002/adfm.201302058

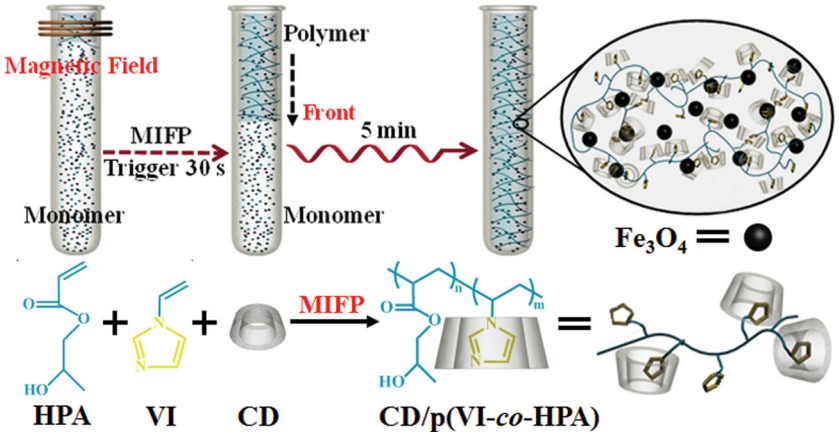


**Figure 1.** Schematic preparation of gels **1** via MIFP and the host-guest assembly in the supramolecular gels. An appropriate amount of $Fe_3O_4$, VI, HPA, CD, MBAA, APS, and TMEDA in the presence of glycerol were added and stirred vigorously at ambient temperature in order to obtain a homogeneous mixture. The final mixture was transferred to a tailored tube-like reactor (15 mL; 10 mm diameter). After triggered via external magnetic stimuli (450 kHz) for only 30 s, the typical front commences propelling. Within 5 min without any treatment, gels were then successfully formed.

between the resultant polymer and unreacted monomer was formed. Within 5 min without any treatment, $Fe_3O_4$-doped CD/p(VI-*co*-HPA) supramolecular gels (**1**) were done. Also prepared were $Fe_3O_4$-doped CD/p(VI-*co*-HPA) supramolecular gels (**2**) and CD/p(VI-*co*-HPA) supramolecular gels (**3**) by a similar polymerization mode triggered by local contact heat source, namely thermal frontal polymerization (TFP), for comparison (see Supporting Information Figure S2 and S3).

Frontal polymerization (FP)[30–33] is a reaction mode of converting the reagents to the products via the propagation of a localized reaction zone through the whole system. After a brief excitation with an external stimulus, no further energy is required in the subsequent reaction process. This reaction mode also offers the advantages of facility and rapidness, and hence has evoked numerous attentions since its discovery. Till now, all the FP in available literatures can be classified into four types with different triggering modes: isothermal frontal polymerization,[34] TFP,[35–38] photo-initiated frontal polymerization[39,40] and plasma-ignited frontal polymerization.[41,42] With dispersion of superparamagnetic particles into monomers, MIFP was created with combination of FP and magnetocaloric effect, where an increase of the applied magnetic field leads to a decrease in magnetic entropy of superparamagnetic particles to generate heat spreading from magnetic system to the environment (monomers) (see Supporting Information). Unlike existing FP triggered by local contact heat source, the new mode of MIFP is induced noncontactly.

The kinetic parameters in MIFP and TFP were analyzed. As shown in Figure S4, both gels **1–3** have been prepared in a quite rapid fashion, and the variation of the CD/VI ratios can easily tune the preparation parameters of both MIFP and TFP modes. With same amount of the reactants but different triggering mode, MIFP of gels **1** behave superior reaction parameters (velocity and temperature) than those for TFP of gels **2**. Therefore, MIFP not only possesses the traditional FP characteristics of high energy saving and fast synthesis in minutes, but also combines magnetocaloric effect to develop a new category of FP to provide a noncontact triggering platform for rapid fabrication of diverse polymers (see Supporting Information). These facile polymerization modes of MIFP and TFP also benefit the host-guest assembly in supramolecular gels.

### 2.2. Host–Guest Assembly in Supramolecular Gels

The host-guest assembly of CD and imidazole groups in supramolecular gels was investigated for the first time. The $^1$H NMR spectra of pure CD, p(VI-*co*-HPA) and gel **3** are shown in **Figure 2**a. An upfield shift of the inside CD protons H-3 and H-5 for gel **3** is observed obviously in comparison with those of pure CD, which may prove the construction of inclusion complex with CD as host and imidazole groups as guest.[43–45] Figure 2b exhibits $^1$H NMR behaviors for gels **3** with different CD/VI ratios under downfield. As the CD/VI ratio increases from 0:10 to 4:10 w/w, clear downfield shifts in the $^1$H NMR signals assigned to the imidazole ring are observed. This variation could be attributed to the supramolecular interaction of imidazole ring and CD that the nitrogen heterocyclic protons in VI undergoes a shielding as CD elevates to form deeper inclusion of host and guest. Figure 2c depicts the FTIR spectra of gel **3**, along with those of pure CD, p(VI-*co*-HPA). After the introduction of CD, the characteristic absorption peaks of imidazole ring at 1261 cm$^{-1}$ (ring vibration) and 1090 cm$^{-1}$ (in-plane ring C-H bending) almost disappear, and its other characteristic absorption at 920 cm$^{-1}$ (out-of-plane ring C-H bending) and 664 cm$^{-1}$ (torsion stretching) weakens to a great degree. The host restriction of vibration of imidazole ring within the cavity of CD could lower the energy of the included part of VI, thereby reducing the intensity of the corresponding absorption bands.[46–49] Meanwhile, a broad band emerges at 1166 cm$^{-1}$, which corresponds to the asymmetric glycoside vibration. Another FTIR analysis was carried out to evaluate the effect of $Fe_3O_4$ nanoparticles on supramolecular networks (Figure 2d). Except one more distinct absorption for Fe-O band at 562 cm$^{-1}$ in gel **1** and gel **2**, there is no obvious difference between FTIR spectra of gels **1–3**, suggesting that the doped $Fe_3O_4$ didn't interfere with the host-guest supramolecular architectures.

To further get insight into the host-guest assembly, some control experiments were carried out. The addition of CD into the other reactant mixture at beginning of and after 2h reaction stage, respectively, afforded gels **4** and **5**, respectively. The $^1$HNMR spectra show that the C–H proton of the imidazole unit undergoes a clear downfield shift for gel **4** (Figure 2e), whereas, the signals of the C–H proton inside CD for **5** can be observed obiviously, which move further upfield than that of **4**. The results reveal better host-guest assembly of CD and imidazole groups in **5** than in **4**. Thermogravimetric analysis (TGA)/FT-IR spectra were also used to record the pyrolysis procedure

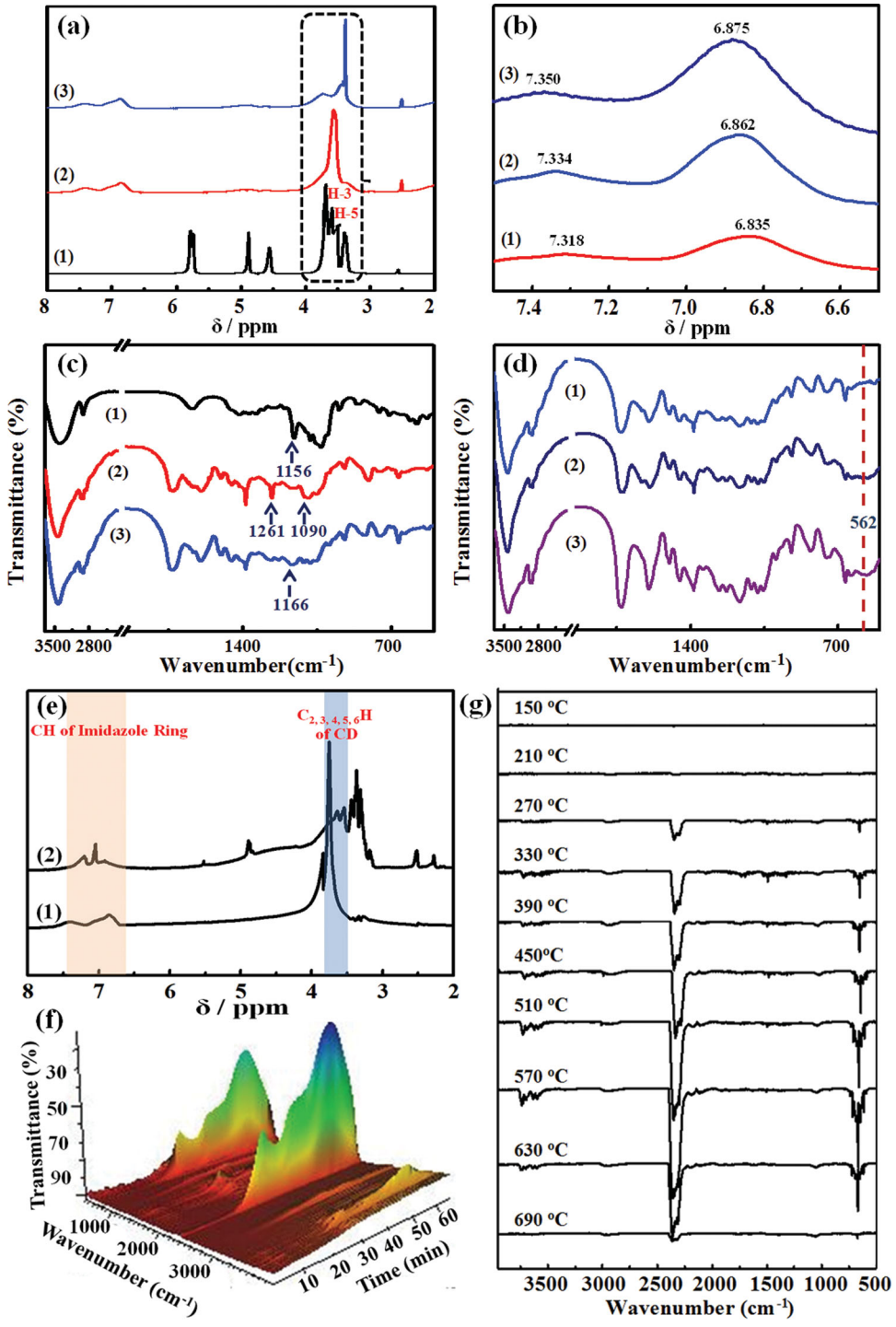


**Figure 2.** a) $^1$H NMR spectra of 1) pure CD, 2) p(VI-*co*-HPA) and 3) gel **3** in DMSO-$d_6$ at 30 °C. b) $^1$H NMR spectral changes of gels **3** with different CD/VI ratios in $D_2O$: 1) 0:10 w/w, 2) 2:10 w/w, 3) 4:10 w/w. c) FTIR spectra of 1) pure CD, 2) p(VI-*co*-HPA) and 3) gel **3**. d) FTIR spectra of 1) gel **3**, 2) gel **1** and 3) gel **2**. e) $^1$H NMR spectra of 1) gel **4** and 2) gels **5** in DMSO-$d_6$ at 20 °C. f) 3D FT-IR profile (150 to 690 °C) and g) the evolutionary FT-IR spectra (150 to 690 °C) of the gases produced from gels **5**.

of supermolecular gels. From the 3D FT-IR profile of gel **5** (Figure 2f), we can see that $CO_2$ (2358 cm$^{-1}$ and 669 cm$^{-1}$) gas is produced early at 230 °C (19 min). The $CO_2$ content gradually elevates with the heating temperature and reaches the highest at ca. 570 °C. $NH_3$ (965 cm$^{-1}$ and 931 cm$^{-1}$) and $H_2O$ (3593 cm$^{-1}$) gases are also released from gel **5**. The details can be detected in the evolutionary FT-IR spectra (Figure 2g). In comparison, gel **4** starts to produce gases at ca. 210 °C (17 min), and the maxmum value of gas content is achieved at ca. 510 °C (see Supporting Information Figure S7). The higher

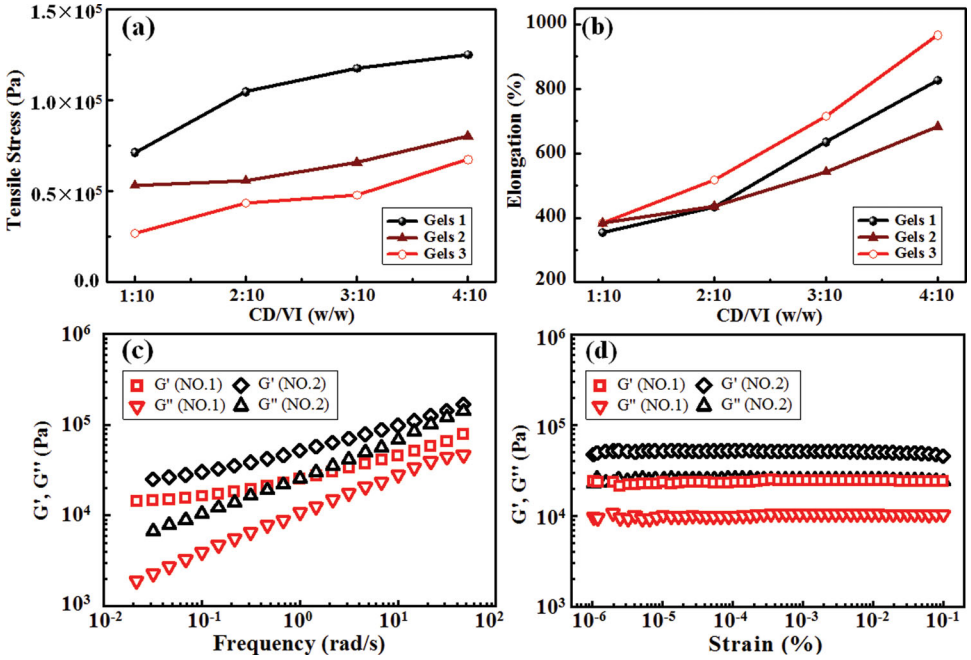


**Figure 3.** a) Tensile stresses and b) elongations versus different CD/VI ratios for gels **1**–**3**. c,d) Storage modulus (*G′*) and loss modulus (*G″*) values of gels **1** c) on frequency sweeps and d) on strain sweeps. No.1: in the absence of CD; No.2: CD/VI = 2:10 w/w.

thermal stability for gel **5** was further confirmed by TGA curves (see Supporting Information, Figure S8). Thus, the addition of CD at the beginning of reaction stage facilitates the formation of host-guest supermolecular network, and the dynamic assembly of VI and CD proceeds simultaneously with the free radical copolymerization of VI and HPA, rather than the occurrence of host-guest interaction afterwards the synthesis of p(VI-*co*-HPA).

### 2.3. Mechanical Properties of Gels 1–3

We systematically investigated the mechanical properties of supramolecular gels. A series of stress–strain experiments were carried out for gels **1**–**3** with different CD/VI ratios of 1:10, 2:10, 3:10, and 4:10 w/w (**Figure 3**a,b). Generally, for all three types of supramolecular gels, the mechanical properties are greatly reinforced upon incorporation of CD. For instance, the tensile strength of gel **1** with CD/VI ratio of 1:10 w/w ($7.1 \times 10^4$ Pa) is nearly three times that of the one without CD ($2.4 \times 10^4$ Pa, see Supporting Information Table S1). Moreover, increasing the concentration of CD gives rise to a remarkable improvement in the stress intensity as well as in the elongation to break. When CD/VI weight ratio increases from 1:10 to 4:10, stress intensity increases from $7.1 \times 10^4$ to $1.25 \times 10^5$ Pa for **1**, from $5.3 \times 10^4$ to $7.0 \times 10^4$ Pa for **2**, and from $2.7 \times 10^4$ to $6.7 \times 10^4$ Pa for **3** (Figure 3a). We can see that the tensile strengths of gels **1** are more than double those of gels **3**, indicating that the introduction of $Fe_3O_4$ nanoparticles improves the mechanical performance of supramolecular gels. Meanwhile, gels **1**–**3** with CD/VI = 4:10 w/w show the elongation at break over 826%, 683%, 967%. The results reveal that the host–guest supramolecular gels have good mechanical strength.[50] In addition, the rheological behavior of supramolecular gels was also investigated. The storage modulus (*G′*) and loss modulus (*G″*) of gels **1** with CD/VI of 0:10 and 2:10 w/w are shown in Figure 3c and d, respectively. At a fixed strain ($\gamma = 0.001\%$), gels **1** display frequency-dependent mechanical moduli, with *G′* magnitudes higher than those of *G″* values, which is the typical behavior of polymer gels. Furthermore, the *G′* and *G″* values increase remarkably with the addition of host CD. The reinforcement in mechanical strength might result from the host–guest interaction that increasing the amount of host facilitates the effective supramolecular interaction.

### 2.4. Self-Healing Behavior of Gels 1–3

Gels **1**–**3** possess intrinsic self-healing behavior without assistance of any external stimulus, and gels **1** and **2** exhibit accelerated healing (from 24 to 3 h for **1**, from 30 to 4 h for **2**) with the treatment of an external magnetic field. To evaluate the intrinsic healing behavior of supramolecular gels, the cylindrical samples of 10 mm diameter were mechanically bisected and then the two halves were brought into contact. After several hours, the autonomic fusion of cut surface as well as self-healing occurred at ambient temperature (see **Figure 4**). **Figure 5**a shows the healed sample composed of one block of gel **1** (black) and the other block of gel **3**. The joint between the two blocks is strong enough to sustain vigorous stretching and the healed gel can be stretched from 5.0 to 22.0 cm. Figure 5b shows the tensile modulus as a function of healing time for healed samples of gels **1**–**3** with CD/VI = 2:10 w/w, respectively. It is obvious that the restorability relies greatly on the contact time, and gel **1** showed ca. 95% of healing efficiency after healing time of 28 h to give tensile modulus of $2.82 \times 10^5$ Pa.

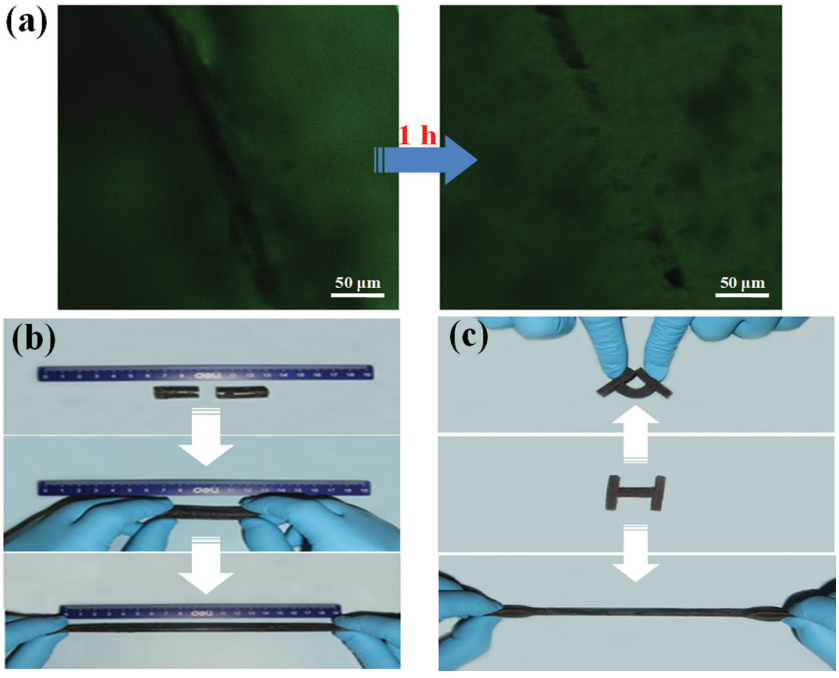


**Figure 4.** a) Fluorescence confocal microscopy images of healing process. The excitation wavelength was 405 nm. b,c) Optical images of gels **1**: b) after cutting into two pieces and attaching the fractured surfaces together for 20 h, the cracks were successfully cured; c) sample was cut into three small blocks and reassemblied into an "H" shape. After pressed for 20 h, the re-contacted block was bent and stretched.

To explore the self-healing mechanism of supramolecular gels, the effect of CD on the healing process was explored. As shown in Figure S9, control samples in the absence of CD have no self-healing ability, revealing that the polymer chains are not long enough to make the functional groups across the welded interface accessible to each other to form hydrogen bond autonomously, analogous to the reported literatures.[51] The self-healing properties of gels **1**–**3** with different CD/VI ratios varying from 1:10 to 4:10 w/w are shown in **Figure 6**a,b. The healing rates of the samples varied significantly as a function of CD contents. With the increase in the CD/VI ratio from 1:10 to 4:10 w/w, the healing time span of gels **1** ranges from 24 to 35 h (Figure 6a). The recovered tensile moduli match well with the virgin mechanical performances of original samples to show healing efficiency > 84% (Figure 6b). Notably, supramolecular gels **1**–**3** with CD/VI = 2:10 w/w reach the maximum values of healing efficiency.

The above investigations suggest that autonomic healing of gels **1**–**3** derives from the host-guest interaction (including hydrogen bonding) between CD and VI segment of polymer, as schematically illustrated in Figure 6c. Firstly, the imidazole group appears to penetrate CD and partly fill the host binding cavity because the imidazole ring possesses the relative smaller size compared to that of hydrophobic interior of CD. Then, according to the size/shape-fit concept, a number of the incompletely filled microstructure are built in this system and distributed along the whole backbone of host-guest gels, while also leads to the mechanical enhancement. Finally, after adjoining the two freshly cut surfaces, the dangling unbound imidazole moieties become increasingly likely to find remaining room to insert CD over time, thus two imidazole moieties might be entrapped and complexed together in the cavity to form an imidazole dimer inclusion complex,[52,53] which leads the non-covalent self-healing to occur. As a result, the equilibrium between the incomplete filled CD and unthreaded VI components is particularly important to achieve the robust and efficient healing, and excess CD could mask the imidazole groups across the polymer chain to induce a decrease in healing efficiency.[24] For instance, as shown in Figure 6b, increasing CD/VI ratio from 2:10 to 4:10 w/w causes the decrease of tensile modulus recovery from 95 to 85% for gels **1**, from 91 to 84% for gels **2** and from 97 to 87% for gels **3**, respectively.

To further confirm the proposal of auto-healing mechanism, results of another experiment are plotted as a function of the fractions of the copolymer components. As illustrated in Supporting Information Figure S10, as the VI/HPA ratio decreases from 2:1 to 1:2 mol/mol, a decrease in healing efficiency from >90% to <65% was observed for gels **1**, respectively, along with an increase in healing time. This observation suggests that the resultant supramolecular gels can still heal themselves to some degree owing to the interlocked host-guest linking in the rejoined area, while the reduced content of imidazole ring guest diminishes the healing rate and efficiency. In addition, after the cut-ends of the gel samples were immersed into high concentration of either VI or CD for hours, they couldn't stick together any more, further supporting our hypothesis.

Significantly, accelerated healing was observed for gels **1** and **2** under an external magnetic field. Two separated parts of the gel sample were attached and the joint region was exposed to a magnetic field (450 kHz)

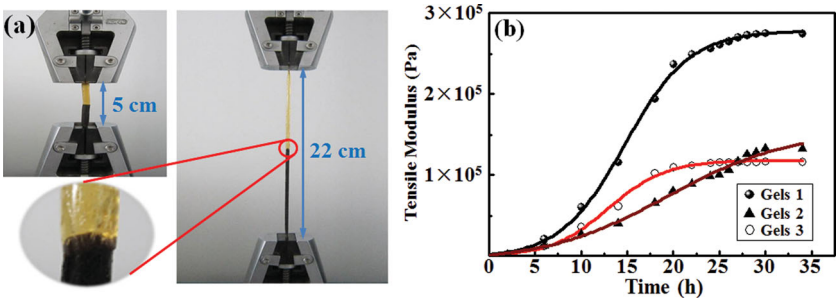


**Figure 5.** a) Stretching processes of a healed sample composed of one block of gel **1** (black) and the other block of gel **3** (yellow) during the tensile measurements. b) Recovery of the tensile modulus versus time for the rejoined samples of gels **1**–**3** with CD/VI = 2:10 w/w.

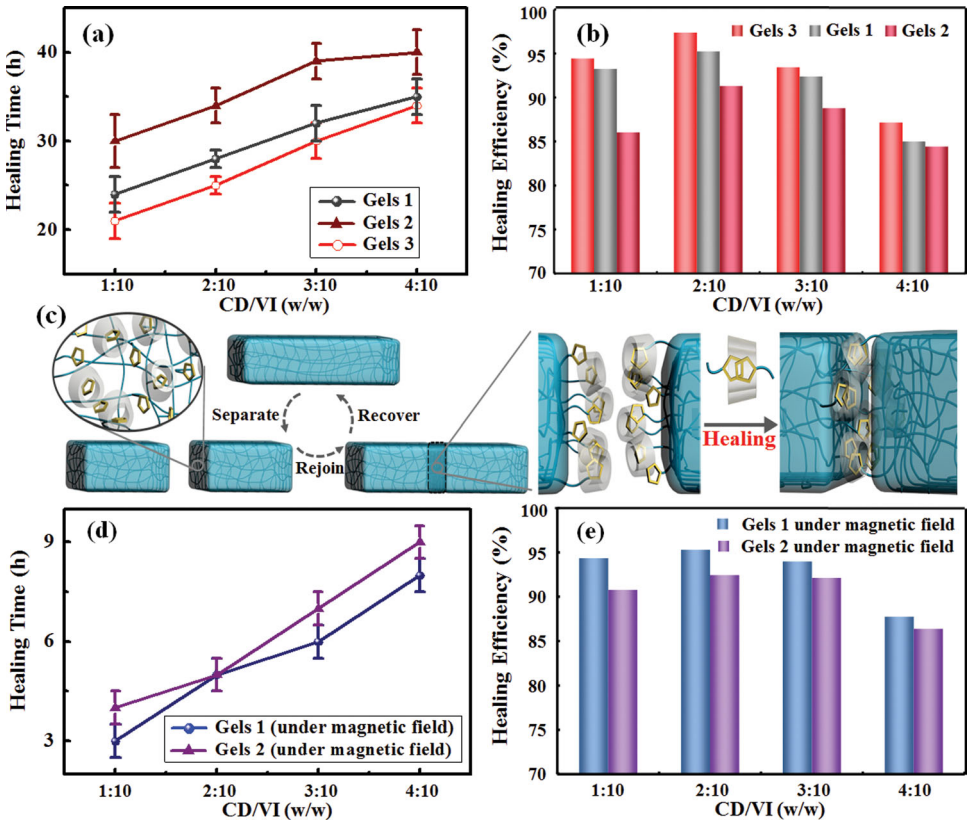


**Figure 6.** a,b) Plots of a) healing time and b) recovery of the tensile modulus versus CD/VI ratios for gels **1**–**3**. The standard deviation is ca. 2. c) Schematic illustration of the self-healing procedure. d,e) Plots of d) healing time and e) recovery of the tensile modulus versus CD/VI ratios for gels **1** and **2** under an external magnetic field. The standard deviation is ca. 3.

for a given time (1–10 h). Then accelerated healing was realized. For samples with CD/VI = 1:10 w/w, the healing time decreased from 24 h to 3 h for **1** and from 30 to 4 h for **2** after applied an external magnetic field (Figure 6a,d). The healing rate of gels under magnetic stimulus is 6 times in average that without magnetic stimulus. More interesting, the increased healing rate doesn't compromise the healing efficiency. As shown in Figure 6e, healed samples show excellent healing efficiency up to 95% for **1** and 92% for **2**, respectively. Furthermore, the healing efficiency of treated samples depends on the ratios of CD/VI, which first lifts and then drops when the weight ratios of CD/VI exceed 2:10 w/w. This feature is consistent with that for gels untreated by magnetic field (Figure 6b), indicating the dominant host-gust interaction for healing process. Furthermore, the oriented migration of $Fe_3O_4$ nanoparticles toward the center of magnet field might cause an amorphous flow of gels in the joint region,[54] which should benefit the host-guest stitches to accelerate self-healing (see Supporting Information Figure S11). Meanwhile, the rejoined control samples of gels **1** kept at 50, 60, 70, 80, and 90 °C in the absence of the applied magnetic field show no considerable change in the healing capacity, which rules out the temperature influence (see Supporting Information, Figure S12). Therefore, the enhanced healing performance should be ascribed to the synergistic interplay between supramolecular assembly and magnetic-induced amorphous flow.

## 3. Conclusions

We demonstrate herein the first fabrication of host-guest supramolecular gels with self-repair capability through a noncontact rapid procedure of magnetically induced frontal polymerization (MIFP) within a few minutes. New type of eco-friendly supramolecular gels are formed by the assembly of "host" *β*-cyclodextrin (CD) and "guest" *N*-vinylimidazole (VI). The resultant supramolecular gels shows noticeable automatic self-healing with healing efficiency of ca. 95%, ascribed to the host-guest interaction between CD and VI. The supramolecular gels also possess high mechanical strength with stress intensity of ca. $1.25 \times 10^5$ Pa and the elongation at break over 826%. More interestingly, the magnetic induction forges a link between magnetic-induced healing and supramolecular host-guest assembly, which could remarkably speed up the healing process (6 times on average). The interesting development of method and materials in this work provides a new insight into the rapid fabrication of novel bio-inspired materials for extensive applications.

## 4. Experimental Section

*Materials*: *N*-vinylimidazole (VI), 2-hydroxypropyl acrylate (HPA), glycerol, *N*,*N*′-methylenebisacrylamide (MBAA), and redox couple, ammonium persulfate (APS)/*N*,*N*,*N*′,*N*′-tetramethylethylenediamine (TMEDA) were commercially available and used as received. $\beta$-cyclodextrin (CD) (98%) and superparamagnetic iron oxide nanoparticles ($Fe_3O_4$) (99.5%; 20 nm beads) were received from Aladdin Industrial Corporation and used without any further purification.

*Pot Life of the Reactants*: Pot life, a period of time that the reagents can remain at ambient temperature before spontaneous polymerization, was assessed by leaving the homogeneous reactant mixture at the ambient temperature and observing the system visually when spontaneous polymerization would take place. At typical amount of component, our reacting system is inert at 23 °C and exhibits the pot life of nearly 2 days, whereas, it turns to be very reactive after triggered through external magnetic stimuli (450 kHz) for only several seconds.

*MIFP of Gels 1*: VI, HPA, CD, *N*,*N*′-methylenebisacrylamide (MBAA), persulfate (APS) and $Fe_3O_4$ nanoparticles were mixed in the presence of glycerol and ultrasound-treated to obtain a homogeneous mixture, and then *N*,*N*,*N*′,*N*′-tetramethylethylenediamine (TMEDA) was added. A typical compositions were VI/HPA = 2:1 mol/mol, APS = 0.5 wt%, [APS]/[TMEDA] = 1:4 mol/mol, $Fe_3O_4$ = 8 wt%, MBAA = 0.03 wt%. The resulting mixture was poured into a tube-like reactor. Subsequently, an external magnetic field (450 kHz) was applied above the reactor for about 30 s to supply enough energy to excite the magnetic moment fluctuations to generate heat source, and a travelling front was formed. After 5 min, the reaction was complete.

*TFP of Gels* **2**: In a typical run, the same amount of each component as described above was vigorously mixed to obtain a homogeneous mixture which was then added into a tube-like reactor. Subsequently, the upper layer of the mixture was heated by a soldering iron at a certain temperature until a flat hot propagating front commenced. Several experiments were performed to guarantee the equal trigger temperature of two FP types for a comparatively reliable comparison.

*TFP of Gels* **3**: For comparison, the same amount of reactant except $Fe_3O_4$ as MIFP of gels **1** was mixed until homogenization. The final mixture was poured into a tube-like reactor and the upper layer was triggered by a soldering iron at a certain temperature until a flat hot propelling front commenced.

*Gels* **4**: a beaker was loaded with APS (initiator) and $Fe_3O_4$ (filler) in the presence of glycerol under ultrasound treatment. Then VI, HPA and MBAA were added and stirred vigorously at ambient temperature in order to obtain a homogeneous mixture. Finally, the reductant TMEDA was poured into the mixed solution. It should noted that the composition was VI/HPA = 2:1 mol/mol, APS = 0.5 wt%, [APS]/[TMEDA] = 1:4 mol/mol, MBAA = 0.03 wt%. The final mixture was transferred to a reaction vessel, immersed in a thermostatic oil bath set at 60 °C for 2 h. Without stopping heating, an appropriate amount of CD solution (CD/VI = 2:10 w/w) was poured into the vessel to entirely immerse the resultant polymer for another 2 h. Ultimately, the product was washed with ethanol several times to remove the unreacted monomers, and then the precipitated gels **4** were dried in a vacuum oven for 36 h.

*Gels* **5**: The same amount of each componet including CD (CD/VI = 2:10 wt/wt) as described ablove was vigorously mixed to achieve a homogeneous mixture which was then transferred to a reaction vessel, immersed in an oil bath set at 60 °C for 2 h. Finally, the product was also washed with ethanol several times to remove the unreacted monomers, and then the precipitated gels **5** were dried in a vacuum oven for 36 h.

*Velocity and Temperature Measurements*: The front velocities were determined by measuring the frontal position as a function of time. When pure FP occurred, a constant velocity of the front can be attained, corresponding to a straight line of the frontal position versus time. Temperature profile was determined by measuring the temperature using FlukeTi30 IR thermal imager at a fixed point (the position of 4.3 cm away from the free surface was chosen for consideration in this work), as a function of time. Then a plot of temperature against frontal position was made by multiplying time by frontal velocity.

*Measurements*: Fluorescent images were recorded on the Leica TCS/SP2 confocal microscope system. Magnetic property of gel **1** was examined at room temperature using a Quantum Design MPMS-XL7 SQUID magnetometer. FT-Raman spectra were recorded by Nicolet 6700 FT-IR spectrometer equipped with a NXR FT-Raman module and the research-grade 2.0 w ND:$YVO_4$ laser with wavelength of 1064 $nm^{-1}$ (see Supporting Information Figure S5). The spectra were collected at a resolution of 4 $cm^{-1}$. The structures of the resultant samples were investigated by SEM with a QUANTA 200 (Philips-FEI, Holland) at 30.0 kV. The slices of samples were immersed in deionized water at room temperature for 7 days. During this period, the water was changed daily so that water-soluble materials could be removed and then the samples were dried in a vacuum oven at 60 °C. Dehydrated samples were immersed again in deionized water to swell at room temperature. After that, the samples were freeze-dried for 20 h. Treated samples used for SEM measurement were cut to expose their inner structure (see Supporting Information Figure S6). Fourier transform infrared (FTIR) studies were carried out on a Nicolet-6700 spectrometer from Thermo Electron at room temperature. The powders were ground into a dry KBr disk. In all cases, 32 scans at a resolution of 4 $cm^{-1}$ were used to record the spectra. $^1H$ high-resolution magnetic-angle spinning (HR-MRS) NMR spectra were collected at 400 MHz on a Bruker Avance 400D instrument. Magic Angle Spinning was carried out with 4-mm double bearing rotors of $ZrO_2$ and spinning rates of 3 kHz. The proton 90° pulse was 10 μs and the relaxation delay 1 s. Chemical shifts were referenced to the solvent values ($\delta$ 2.50 ppm for DMSO-$d_6$, and $\delta$ 4.68 ppm for HOD). Thermogravimetric analysis (TGA) curves and the evolutionary FT-IR profiles were collected on a NETZSCH STA 449 F3 Jupiter/Nicolet 6700 (TGA/FT-IR) system. The samples were combusted in the air at the temperature ranging from 40 to 700 °C (10 °C/min).

*Healing of Supramolecular Gels*: For the self-healing tests, two freshly cut surfaces of samples were stuck together and were pressed for ca. 1 min. Afterwards, the rejoined sample was left to self-heal for a certain time at room temperature without any external stimuli. Finally, stress-strain tests were conducted to assess the healing degree of the samples in different contact time.

For $Fe_3O_4$-assisted healing tests, separated samples of gels **1** and **2** were subjected to the same pretreatment and then the incision was positioned in the center of copper coil with a field frequency of 450 kHz for a given time. Finally, the healing efficiency of the samples was confirmed through stress-strain tests. Besides, for controlled experiments the samples were left to repair at 50, 60, 70, 80, and 90 °C. Then, stress-strain tests were conducted to assess the healing degree of the samples in different contact time.

For reproducibility, three parallel measurements for each experiment had to be performed to ensure the reliable data, and the data in the context are mean values.

*Mechanical Testing*: The rheological experiments of the samples were conducted on a HAAKE MARS III instrument using a parallel plate of 20 mm diameter at 30 °C. The mechanical tensile stress versus strain experiments were performed using SANS CMT6203 testing machine at 25 °C. The mechanical properties of cylindrical samples (10 mm diameter) were determined at a crosshead speed of 20 mm/min and the sample length between jaws was set to 50 mm. For reproducibility, each measurement was repeated at least three times and the values were averaged.

*Magnetic Field Application*: Inductive heating was accomplished by placing the sample in the center of a copper coil (30 mm diameter; 3 turns; 4 mm distance between each turn) at an oscillation frequency (f = 450 kHz) and magnetic field amplitude (H = 15 kA/m). The equipment (Supporting Information Figure S12) was composed of a high-frequency generator (GPH-5KW; Deer Electronic, Zhangjiagang, China). An internal cooling system was used to provide cycle water for the coil, and the Fluke Ti30 IR thermal imager was fixed a point at a certain distance from the coil for noncontact measuring temperature of the samples.

## Supporting Information

Supporting Information is available from the Wiley Online Library or from the author.

## Acknowledgements

This work was supported by the National Natural Science Foundation of China (21006046 and 21076103), Natural Science Foundation of Jiangsu (BK20131408), Natural Science Foundation for Jiangsu Higher Education Institutions of China (10KJB530006), National High Technology Research and Development Program of China (863 Program) (2012AA030313), and Priority Academic Program Development of Jiangsu Higher Education Institutions (PAPD).

Received: June 16, 2013
Revised: July 19, 2013
Published online: September 23, 2013

[1] H. Ceylan, M. Urel, T. S. Erkal, A. B. Tekinay, A. Dana, M. O. Guler, *Adv. Funct. Mater.* **2013**, *23*, 2081.
[2] M. J. Barthel, T. Rudolph, A. Teichler, R. M. Paulus, J. Vitz, S. Hoeppener, M. D. Hager, F. H. Schacher, U. S. Schubert, *Adv. Funct. Mater.* **2013**, DOI: 10.1002/adfm.201300469.
[3] B. C. K. Tee, C. Wang, R. Allen, Z. N. Bao, *Nat. Nanotechnol.* **2012**, *7*, 825.
[4] T. S. Coope, U. F. J. Mayer, D. F. Wass, R. S. Trask, I. P. Bond, *Adv. Funct. Mater.* **2011**, *21*, 4624.
[5] M. Burnworth, L. M. Tang, J. R. Kumpfer, A. J. Duncan, F. L. Beyer, G. L. Fiore, S. J. Rowan, C. Weder, *Nature* **2011**, *472*, 334.
[6] J. H. Park, P. V. Braun, *Adv. Mater.* **2010**, *22*, 496.
[7] B. Ghosh, M. W. Urban, *Science* **2009**, *323*, 1458.
[8] S. R. White, N. R. Sottos, P. H. Geubelle, J. S. Moore, M. R. Kessler, S. R. Sriram, E. N. Brown, S. Viswanathan, *Nature* **2001**, *409*, 794.
[9] M. D. Ward, P. R. Raithby, *Chem. Soc. Rev.* **2013**, *42*, 1619.
[10] J. Fox, J. J. Wie, B. W. Greenland, S. Burattini, W. Hayes, H. M. Colquhoun, M. E. Mackay, S. J. Rowan, *J. Am. Chem. Soc.* **2012**, *134*, 5362.
[11] S. Burattini, B. W. Greenland, D. H. Merino, W. G. Weng, J. Seppala, H. M. Colquhoun, W. Hayes, M. E. Mackay, I. W. Hamley, S. J. Rowan, *J. Am. Chem. Soc.* **2010**, *132*, 12051.
[12] J. Hentschel, A. M. Kushner, J. Ziller, Z. B. Guan, *Angew. Chem. Int. Ed.* **2012**, *51*, 10561.
[13] Y. L. Chen, A. M. Kushner, G. A. Williams, Z. B. Guan, *Nat. Chem.* **2012**, *4*, 467.
[14] X. Wang, F. Liu, X. W. Zheng, J. Q. Sun, *Angew. Chem. Int. Ed.* **2011**, *50*, 11378.
[15] Q. Wang, J. L. Mynar, M. Yoshida, E. Lee, M. Lee, K. Okuro, K. Kinbara, T. Aida, *Nature* **2010**, *463*, 339.
[16] D. C. Tuncaboylu, M. Sari, W. Oppermann, O. Okay, *Macromolecules* **2011**, *44*, 4997.
[17] G. Q. Jiang, C. Liu, X. L. Liu, G. H. Zhang, M. Yang, F. Q. Liu, *Macromol. Mater. Eng.* **2009**, *294*, 815.
[18] T. Kakuta, Y. Takashima, M. Nakahata, M. Otsubo, H. Yamaguchi, A. Harada, *Adv. Mater.* **2013**, *25*, 2849.
[19] M. Zhang, D. Xu, X. Yan, J. Chen, S. Dong, B. Zheng, F. Huang, *Angew. Chem. Int. Ed.* **2012**, *51*, 7011.
[20] M. Nakahata, Y. Takashima, H. Yamaguchi, A. Harada, *Nat. Commun.* **2011**, DOI: 10.1038/ncomms1521.
[21] Z. Liu, M. Frasconi, J. Lei, Z. J. Brown, Z. Zhu, D. Cao, J. Iehl, G. Liu, A. C. Fahrenbach, Y. Y. Botros, O. K. Farha, J. T. Hupp, C. A. Mirkin, J. Fraser Stoddart, *Nat. Commun.* **2013**, *4*, 1855.
[22] Y. Zheng, A. Hashidzume, Y. Takashima, H. Yamaguchi, A. Harada, *Nat. Commun.* **2012**, DOI: 10.1038/ncomms1841.
[23] G. Izzet, M. Menand, B. Matt, S. Renaudineau, L. M. Chamoreau, M. Sollogoub, A. Proust, *Angew. Chem. Int. Ed.* **2012**, *51*, 487.
[24] A. Harada, R. Kobayashi, Y. Takashima, A. Hashidzume, H. Yamaguchi, *Nat. Chem.* **2011**, *3*, 34.
[25] G. Chen, M. Jiang, *Chem. Soc. Rev.* **2011**, *40*, 2254.
[26] P. Nordblad, *Nat. Mater.* **2013**, *12*, 11.
[27] B. Mehdaoui, A. Meffre, J. Carrey, S. Lachaize, L. M. Lacroix, M. Gougeon, B. Chaudret, M. Respaud, *Adv. Funct. Mater.* **2011**, *21*, 4573.
[28] B. J. Adzima, C. J. Kloxin, C. N. Bowman, *Adv. Mater.* **2010**, *22*, 2784.
[29] T. Hoare, J. Santamaria, G. F. Goya, S. Irusta, D. Lin, S. Lau, R. Padera, R. Langer, D. S. Kohane, *Nano Lett.* **2009**, *9*, 3651.
[30] N. M. Chechilo, R. J. Khvilivitskii, N. S. Enikolopyan, *Dokl. Akad. Nauk. SSSR* **1972**, *204*, 1180.
[31] P. M. Goldfeder, V. A. Volpert, V. M. Ilyashenko, A. M. Khan, J. A. Pojman, S. E. Solovyov, *J. Phys. Chem. B* **1997**, *101*, 3474.
[32] A. Tredici, R. Pecchini, M. Morbidelli, *J. Polym. Sci. Pol. Chem.* **1998**, *36*, 1117.
[33] Y. Koike, H. Hatanaka, Y. Ohtsuka, *Appl. Optics* **1984**, *23*, 1779.
[34] A. Mariani, D. Nuvoli, V. Alzari, M. Pinf, *Macromolecules* **2008**, *41*, 5191.
[35] Q. Z. Yan, G. D. Lu, W. F. Zhang, X. H. Ma, C. C. Ge, *Adv. Funct. Mater.* **2007**, *17*, 3355.
[36] R. P. Washington, O. Steinbock, *J. Am. Chem. Soc.* **2001**, *123*, 7933.
[37] J. A. Pojman, *J. Am. Chem. Soc.* **1991**, *113*, 6284.
[38] J. V. Crivello, *J. Polym. Sci. Pol. Chem.* **2007**, *45*, 4331.
[39] J. V. Crivello, R. Falk, M. R. Zonca, *J. Polym. Sci. Pol. Chem.* **2004**, *42*, 1630.
[40] J. Zhou, H. A. Shao, J. Tu, Y. A. Fang, X. Guo, C. F. Wang, L. Chen, S. Chen, *Chem. Mater.* **2010**, *22*, 5653.
[41] C. Yu, J. Zhou, C. F. Wang, L. Chen, S. Chen, *J. Polym. Sci. Pol. Chem.* **2011**, *49*, 52176.
[42] B. G. Shen, J. R. Sun, F. X. Hu, H. W. Zhang, Z. H. Cheng, *Adv. Mater.* **2009**, *21*, 4545.
[43] S. Bekiroglu, L. Kenne, C. Sandstrom, *J. Org. Chem.* **2003**, *68*, 1671.
[44] G. R. Goward, M. F. H. Schuster, D. Sebastiani, I. Schnell, H. W. Spiess, *J. Phys. Chem. B* **2002**, *106*, 9322.
[45] H. J. Schneider, F. Hacket, V. Rudiger, H. Ikeda, *Chem. Rev.* **1998**, *98*, 1755.
[46] W. Sajomsang, O. Nuchuchua, P. Gonil, S. Saesoo, I. Sramala, A. Soottitantawat, S. Puttipipatkhachorn, U. R. Ruktanonchai, *Carbohyd Polym.* **2012**, *89*, 623.
[47] C. Garnero, V. Aiassa, M. Longhi, *J. Pharmaceut. Biomed.* **2012**, *63*, 74.
[48] A. Celebioglu, T. Uyar, *Langmuir* **2011**, *27*, 6218.
[49] M. X. Zhao, Q. Xia, X. D. Feng, X. H. Zhu, Z. W. Mao, L. N. Ji, K. Wang, *Biomaterials* **2010**, *31*, 4401.
[50] Z. M. Yang, L. Wang, J. Y. Wang, P. Gao, B. Xu, *J. Mater. Chem.* **2010**, *20*, 2128.
[51] A. Phadke, C. Zhang, B. Arman, C. C. Hsu, R. A. Mashelkar, A. K. Lele, M. J. Tauber, G. Arya, S. Varghese, *Proc. Natl. Acad. Sci. U.S.A.* **2012**, *109*, 4383.
[52] B. Chen, K. L. Liu, Z. X. Zhang, X. P. Ni, S. H. Goh, J. Li, *Chem. Commun.* **2012**, *48*, 5638.
[53] W. G. Herkstroeter, P. A. Martic, T. R. Evans, S. Farid, *J. Am. Chem. Soc.* **1986**, *108*, 3275.
[54] C. C. Corten, M. W. Urban, *Adv. Mater.* **2009**, *21*, 5011.